International Journal of Mass Spectrometry 280 (2009) 144–148

Contents lists available at ScienceDirect

International Journal of Mass Spectrometry

journal homepage: www.elsevier.com/locate/ijms

Recombination of HCO^+ and DCO^+ ions with electrons

I. Korolov, R. Plasil*, T. Kotrik, P. Dohnal, J. Glosik

Department of Surface and Plasma Science, Faculty of Mathematics and Physics, Charles University in Prague, V Holešovičkách 2, 180 00 Prague, Czech Republic

ARTICLE INFO

Article history:
Received 9 June 2008
Received in revised form 10 July 2008
Accepted 18 July 2008
Available online 30 July 2008

Keywords:
Plasma
Recombination
HCO^+
DCO^+

ABSTRACT

Recombination of HCO^+ and DCO^+ ions with electrons was studied in afterglow plasma. The flowing afterglow with Langmuir probe (FALP) apparatus was used to measure the recombination rate coefficients and their temperature dependencies in the range 150–270 K. To obtain a recombination rate coefficient for a particular ion, the dependencies on partial pressures of gases used in the ion formation were measured. The variations of $\alpha_{HCO^+}(T)$ and $\alpha_{DCO^+}(T)$ seem to obey the power law: $\alpha_{HCO^+}(T) = (2.0 \pm 0.6) \times 10^{-7} (T/300)^{-1.3}$ cm^3 s^{-1} and $\alpha_{DCO^+}(T) = (1.7 \pm 0.5) \times 10^{-7} (T/300)^{-1.1}$ cm^3 s^{-1} over the studied temperature range.

1. Introduction

The HCO^+ molecular ion is one of the key ions in astrophysically relevant plasmas. In the interstellar medium it is predominantly formed in ion molecule reactions of CO with H_3^+. It is believed that the major destruction mechanism for these ions is dissociative recombination. Observations of both HCO^+ and DCO^+ ions are powerful probes of physical conditions in these plasmas [1–3].

The recombination of HCO^+ ions with low-temperature electrons was studied many times theoretically and also by different experimental techniques. The values of the thermal recombination rate coefficient (at 300 K) obtained by different techniques, such as merged beam study [4], storage ring experiments [5], stationary afterglow [6–8] and flowing afterglow [9–11] are within the range $1–3 \times 10^{-7}$ cm^3 s^{-1}. The apparent agreement at 300 K turns towards disagreement when temperature dependencies are measured. For temperatures below 300 K, the measured recombination rate coefficients differ by nearly one order of magnitude. In some former experiments the possibility of internally excited HCO^+ (DCO^+) ions, including the presence of higher energy isomers HOC^+ (and DOC^+), cannot be excluded. The negative temperature dependencies were observed in many previously reported studies [5–10], but the character of these dependencies was very different. In addition, decrease of recombination rate coefficient with decreasing temperature was obtained in a recent FALP experiment [12]. The mechanism of dissociative recombination of the HCO^+ ion is also very controversial. What is clear is that the recombination of HCO^+ is a multi-step indirect process. It was concluded that the rate-determining step for recombination of HCO^+ is a capture into Rydberg states [13,14]. The most recent calculations [15] have a tendency to decrease the distinctions between theory and experiment. Nevertheless, the calculated thermal value of the recombination rate coefficient is lower by a factor of 10 [14,15] than values obtained in numerous experimental studies [12,16]. The discrepancy is probably caused by the imperfection of theoretical calculations due to a lack of knowledge about modelling the dissociative recombination processes of triatomic ions. Nevertheless, we cannot exclude that the problem lay in the experiments. In a recent study of recombination of H_3^+ it was observed that the measured recombination rate coefficients in plasmatic experiments can be enhanced at a higher pressure of ambient gas [17]. The phenomena is connected with mechanism of H_3^+ recombination [18]. We can expect similar phenomena also for HCO^+ recombination (see Refs. [14,15], see also discussion on H_3^+ and HCO^+ in Ref. [19]); we considered this during our study. In order to confirm or disprove the unexpected temperature dependence observed in the recent FALP experiment [12] and to obtain data about recombination of DCO^+, we carried out well-defined experiments using the flowing afterglow technique (FALP). Having in mind a recent observation of ternary recombination in H_3^+ and D_3^+ dominated plasma [17], we also measured the pressure dependence of recombination rate coefficients of HCO^+ and DCO^+ ions. In addition, attention was paid to processes of formation of plasma dominated by the studied ions in order to exclude the influence of high-energy isomers

* Corresponding author. Tel.: +420 221 912 224; fax: +420 284 685 095.
E-mail address: radek.plasil@mff.cuni.cz (R. Plasil).

1387-3806/$ – see front matter © 2008 Elsevier B.V. All rights reserved.
doi:10.1016/j.ijms.2008.07.023

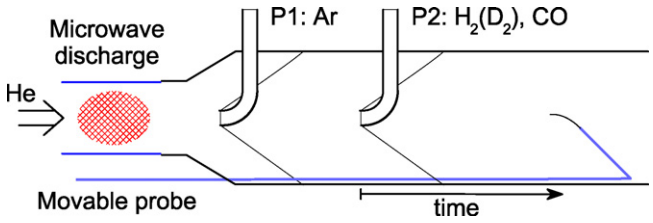

Fig. 1. The principle of FALP experiment. The plasma is formed in a microwave discharge and then is driven by the flow of helium along the flow tube (from left to right in the drawing). The reactant gases (indicated for present experiments) are added via ports P1 and P2 to form plasma dominated by the desired ions. The plasma parameters are measured by a Langmuir probe movable along the flow tube from the position of port P2 to the end of the flow tube. We set the time scale origin at the position of port P2; $t_{P2} = 0$.

HOC^+ and DOC^+ in decaying plasma on measured recombination rate coefficients.

2. Experiment

2.1. Experimental details

The principle of the flowing afterglow method used in present FALP experiments is described in Fig. 1; the details are given elsewhere [20–23]. In a FALP experiment, helium buffer gas flows along the flow tube. There is a glass section in the upstream part of the flow tube where plasma is generated by microwave discharge (~15 W). The flowing helium then drives plasma into a stainless steel section of the flow tube (internal diameter ~5 cm). The plasma leaving the discharge region contains He^+ ions, electrons and long-living helium metastables ($He(2^3S)$ and $He(2^1S)$) [20,24,25]. Because of high-He pressure (1200–2000 Pa), He^+ ions are rapidly converted to He_2^+ ions in a three-body association process (for description of kinetics in the He afterglow see Ref. [26] and references therein). Downstream from the discharge region, Ar is added to the flow tube. After an addition of Ar (via port P1), helium metastables are removed from the plasma by Penning ionisation and Ar^+ ions and electrons are formed. The He_2^+ ions also react with Ar and Ar^+ ions are formed. When the metastables are removed the Ar^+ dominated plasma rapidly relaxes. The processes of relaxation in the flow tube are clear, well described and documented [20,22,24,26]. Further reactant gases can be added to the afterglow plasma via port P2 to form plasma dominated by the desired ion. To minimise the level of impurities, helium is purified by passing through a zeolite trap cooled by liquid nitrogen. The obtained impurity level of He in the flow tube is below 0.1 ppm. The flow tube is cooled to 250 K to suppress partial pressure of water vapour. The parameters of the plasma decaying along the flow tube are monitored by an axially movable Langmuir probe (7 mm long tungsten wire of diameter 18 μm). Probe characteristics (current to voltage) are measured at different positions along the flow tube. The corresponding electron number densities (n_e) are determined from the "electron saturated region" of measured probe characteristics. To obtain absolute values of electron densities, the probe is calibrated by measuring well-established recombination rate coefficients of O_2^+ ions [16,26]. In fact, the calibration just confirms the accuracy of the electron density measurements based on probe theory [27]. Further relevant information connected with application of a Langmuir probe in flowing afterglow and justification of used method is given in Refs. [10,22,24,28,29].

The buffer gas velocity gives the relation between the decay time and the position. The actual plasma velocity on the axis of the flow tube is measured by a modulation of the discharge and by monitoring the propagation of the distortion along the flow tube.

Table 1
The main reactions considered as leading to the formation and destruction of HCO^+ ions

No.	Reaction	Rate coefficient ($cm^3\ s^{-1}$)	Reference
1	$Ar^+ + H_2 \rightarrow ArH^+ + H$ $Ar^+ + H_2 \rightarrow Ar + H_2^+$	8×10^{-10} 1×10^{-10}	[33]
2	$H_2^+ + Ar \rightarrow ArH^+ + H$	2.3×10^{-9}	[34]
3	$H_2^+ + H_2 \rightarrow H_3^+ + H$	2.1×10^{-9}	[34]
4	$ArH^+ + H_2 \rightarrow H_3^+ + Ar$	1.5×10^{-9}	[34]
5	$ArH^+ + CO \rightarrow HCO^+ + Ar$ $ArH^+ + CO \rightarrow HOC^+ + Ar$	1.25×10^{-9}	[35]
6	$Ar^+ + CO \rightarrow CO^+ + Ar$	4×10^{-11}	[36]
7	$CO^+ + H_2 \rightarrow HOC^+ + H$ (48%) $CO^+ + H_2 \rightarrow HCO^+ + H$	1.5×10^{-9}	[30]
8	$H_2^+ + CO \rightarrow HCO^+ + H$	$>1 \times 10^{-9}$	[6]
9	$H_3^+ + CO \rightarrow HOC^+ + H_2$ (6%) $H_3^+ + CO \rightarrow HCO^+ + H_2$	1.4×10^{-9}	[6]
10	$HOC^+ + H_2 \rightarrow HCO^+ + H_2$	4.7×10^{-10}	[30]
11	$HOC^+ + CO \rightarrow HCO^+ + CO$	6×10^{-10}	[30]
12	$HCO^+ + e^- \rightarrow$ products	2.5×10^{-7}	This work
13	$CO^+ + e^- \rightarrow C + O$	2×10^{-7}	[37]
14	$HOC^+ + e^- \rightarrow H + CO$	1.3×10^{-7}	[38]

The rate coefficients are specified for 300 K. The reactions leading to the formation of Ar^+ dominated plasma prior to the port P2 are not listed; for corresponding reactions see, e.g., [26]. The detailed discussion about the reactions leading to the formation of HCO^+ dominated plasma is given in Ref. [32].

Under the used experimental conditions, we can monitor plasma decay over 60 ms. From the decay of the electron density along the flow tube, the recombination rate coefficient and characteristic diffusion time are calculated. An advanced data analysis procedure was used to obtain the recombination rate coefficients. The advanced data analysis method allows us to determine precisely the formation/mixing region and to calculate the proper value of the recombination rate coefficient (see discussion below and the discussion in Refs. [22,26]).

2.2. Formation of plasmas dominated by HCO^+ and DCO^+ ions and their decay

There are several possible reaction routes for creating the studied ions. Reactions leading to the formation of HCO^+ are listed in Table 1. Formation of DCO^+ is similar, so it will be not discussed further. Note that in some reactions, metastable HOC^+ isomer ions are formed as well. Nevertheless, they immediately react with H_2 or CO (exothermic catalytic isomerisation; for more detailed information see [30] and [31]):

$$HOC^+ + H_2 \rightarrow HCO^+ + H_2 \quad \text{and} \quad HOC^+ + CO \rightarrow HCO^+ + CO$$

Since the rates of isomerization of HOC^+ are relatively high, the HOC^+ ions will be converted into the lowest energy isomers in a few milliseconds under our conditions and therefore they cannot influence the measurement of the recombination rate coefficient of HCO^+ ions.

In order to optimise experimental conditions and to understand details of processes in the afterglow, the evolution of partial densities of ions along the flow tube were calculated using a numerical kinetic model. The actual experimental conditions (plasma velocity, pressure, the partial pressures of reactants, geometry of the flow tube, temperature, etc.) were used in the model. The ambipolar diffusion, recombination loss processes and ion molecule reactions

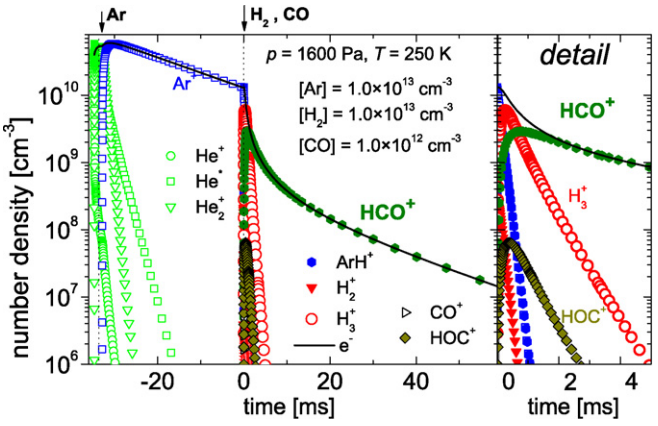

Fig. 2. (Left panel) The calculated ion-formation and plasma decay along the flow tube at conditions typical for the present HCO^+ experiments. (Right panel) A detail of the calculated ion densities near the port P2 where H_2 and CO are added (low-decay time). Conditions: $T = 250$ K, $p = 1600$ Pa. The partial densities of H_2 and CO are written in the figure. The time scale origin is set at the position of port P2, thus times upstream have negative value.

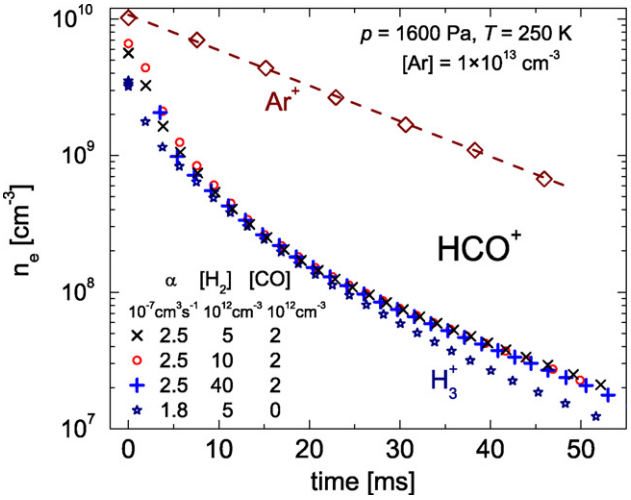

Fig. 3. The examples of electron density decays measured in HCO^+ dominated plasmas at $T = 250$ K and at several hydrogen concentration, $[H_2]$. The obtained recombination rate coefficients are indicated. For the sake of comparison, decay curves measured in H_3^+ and Ar^+ dominated plasmas in otherwise identical conditions are also included in the figure.

were taken into account in the model. Quasi-neutrality of the afterglow plasma is assumed in the model. Results of the calculations obtained for partial densities of reactants used in our experiments are given in Fig. 2.

The numerical model of plasma formation for DCO^+ ions gives similar results as for HCO^+. The data plotted in Fig. 2 indicate that the plasma decay during the first 5 ms after the addition of reactants (see detail in right panel) is influenced by the presence of several ions (Ar^+, HCO^+, H_3^+, HOC^+, etc.). Therefore, to avoid an erroneous estimation of the recombination rate coefficients from the experimental data we took into account the processes in the formation zone. Furthermore, for low concentration of H_2 and higher concentration of CO the plasma decay is influenced mainly by the presence of a high amount of CO^+ ions. We used the kinetic model to calculate ion composition and electron density decays for different H_2 and CO densities. The recombination rate coefficient $\alpha_{HCO^+}(250\,K) = 2.5 \times 10^{-7}\,cm^3\,s^{-1}$ was used in these calculations. From the calculation it is evident that at low-hydrogen (deuterium) concentrations $[H_2] < 2 \times 10^{12}\,cm^{-3}$ the electron density decays are obviously affected by the recombination of both HCO^+ and CO^+ ions. We concluded that at buffer gas pressure 1100–1800 Pa, the appropriate conditions for HCO^+ study are given by the limits: $2 \times 10^{12}\,cm^{-3} \le [H_2] \le 1 \times 10^{14}\,cm^{-3}$, $[CO] \le 5 \times 10^{12}\,cm^{-3}$. The limitation $[H_2] \le 1 \times 10^{14}\,cm^{-3}$ is required by the necessity to exclude the formation of cluster/complex ions [39].

3. Results and discussion

The main goal of the present studies was to measure the temperature and pressure dependencies of the recombination rate coefficients for HCO^+ and DCO^+ ions. The measurements were performed at temperatures 150–270 K. The total buffer gas pressure was maintained at 1200 and 1600 Pa. The measurements were carried out over a wide range of CO and H_2 (D_2) densities. The electron density decays were measured along the flow tube over the distance ~30 cm. The corresponding decay time is ~60 ms (see Fig. 2). Examples of measured electron density decay curves in HCO^+ and DCO^+ dominated afterglow for several densities of H_2 and D_2, respectively are plotted in Figs. 3 and 4.

Together with the HCO^+ and DCO^+ studies the measurements in the He–Ar–H_2 (or D_2) mixture, i.e., without CO, were also performed and the recombination rate coefficients for H_3^+ and D_3^+ were obtained. Note in Fig. 3 that at given conditions, the rate of recombination of H_3^+ ions is comparable with the rate of recombination of HCO^+ ions; for a comparison see Fig. 2 from Smith and Spanel in Ref. [10], or Fig. 7.2 from Ref. [19]. The reason is that the present measurements are at a high pressure (1600 Pa) and recombination of H_3^+ has a ternary channel, which enhances recombination at a higher pressure of ambient gas [17]. The rate coefficients obtained for the recombination of HCO^+ and DCO^+ ions at two different temperatures and two buffer gas pressures are plotted in Fig. 5.

Within the accuracy of the FALP measurements (±30%), the dependence of the measured recombination rate coefficient on helium pressure was not observed. The obtained values of the rate coefficients of recombination of HCO^+ and DCO^+ ions with electrons at temperature 250 K are: $\alpha_{HCO^+}(250\,K) = (2.5 \pm 0.7) \times 10^{-7}\,cm^3\,s^{-1}$ and $\alpha_{DCO^+}(250\,K) = (1.9 \pm 0.6) \times 10^{-7}\,cm^3\,s^{-1}$. The obtained values of these rate coefficients at temperature 180 K are evidently greater than at 250 K (see Fig. 5): $\alpha_{HCO^+}(180\,K) = (3.7 \pm 1.1) \times 10^{-7}\,cm^3\,s^{-1}$ and $\alpha_{DCO^+}(180\,K) = (2.8 \pm 0.8) \times 10^{-7}\,cm^3\,s^{-1}$. Hence, the decrease

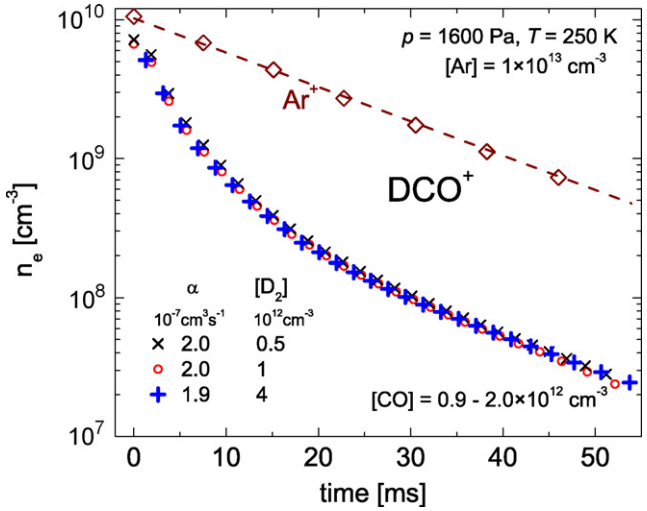

Fig. 4. The examples of electron density decays measured in DCO^+ dominated plasmas along the flow tube. The temperature, pressure and corresponding Ar, D_2 and CO densities are indicated.

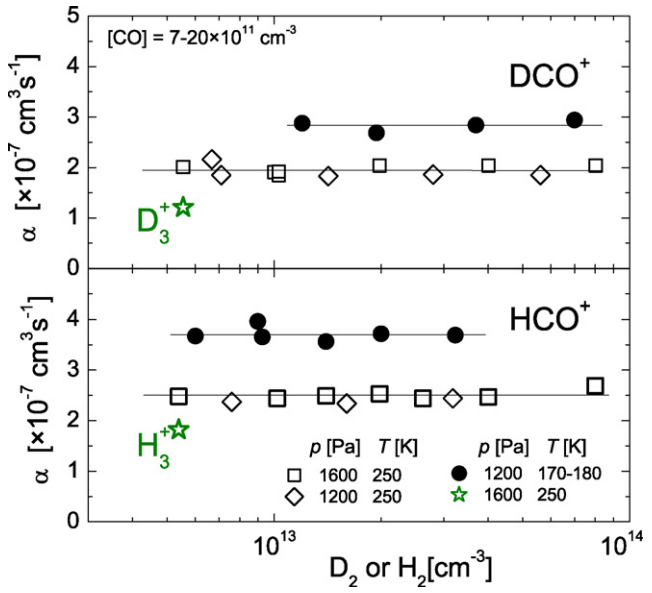

Fig. 5. The recombination rate coefficients measured as a function of H_2 or D_2 densities in HCO^+ (lower panel) and DCO^+ (upper panel) dominated plasmas. The pressure of He and temperatures are indicated. The stars indicate recombination rate coefficients measured in H_3^+ (lower panel) and D_3^+ (upper panel) dominated plasmas (without addition of CO).

of the rate coefficients at temperatures below 300 K reported in [12] was not observed. The dependence of the recombination rate coefficient of DCO^+ on temperature is plotted in Fig. 6. Over the studied temperature range (150–270 K), the variation of $\alpha_{DCO^+}(T)$ seems to obey the power law of $T^{-\beta}$. Therefore, the experimental data were fitted using the following equation in order to determine β: $\alpha(T) = \alpha(300\,\mathrm{K})(T/300\,\mathrm{K})^{-\beta}$, where $\alpha(300\,\mathrm{K})$ and β are the parameters. After fitting the experimental data, the following β and $\alpha(300\,\mathrm{K})$ were determined for HCO^+ and DCO^+ recombination:

$$HCO^+ : \alpha_{HCO^+}(300\,\mathrm{K}) = (2.0 \pm 0.3) \times 10^{-7}\,\mathrm{cm^3\,s^{-1}} \quad \text{and}$$
$$\beta = 1.3 \pm 0.2$$

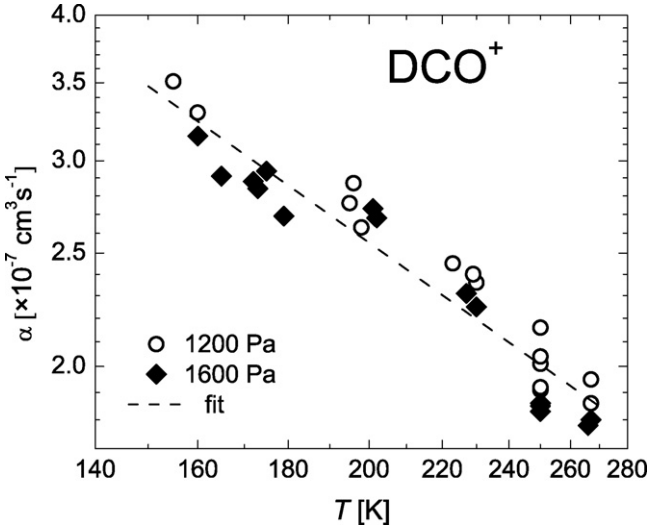

Fig. 6. The temperature dependence of the recombination rate coefficient of DCO^+ ions measured in FALP experiment. The corresponding buffer gas pressures are indicated.

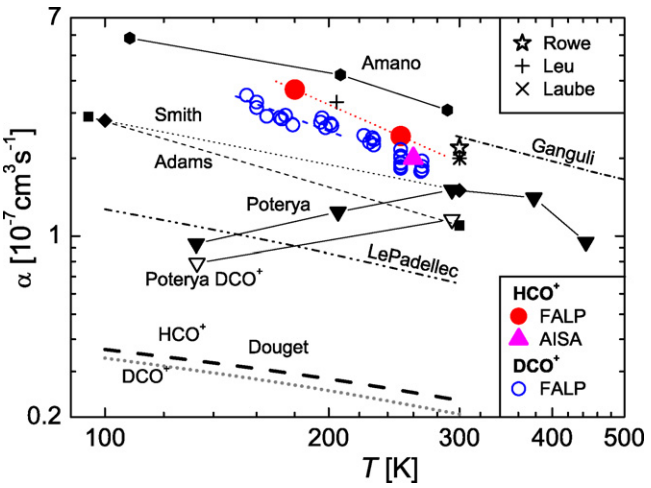

Fig. 7. The recombination rate coefficients of HCO^+ and DCO^+ ions measured in different experiments. Recent theoretical values (Douguet et al. [15]) are also indicated. For an overview, there are recent experimental values plotted: Amano [7], Rowe et al. [11], Leu et al. [6], Laube et al. [41], Ganguli et al. [8], Smith and Spanel [10], Adams et al. [9] and Poterya et al. [12]. The values from reference Le Padellec et al. [4] are corrected in accordance with discussion in Ref. [19].

$$DCO^+ : \alpha_{DCO^+}(300\,\mathrm{K}) = (1.7 \pm 0.3) \times 10^{-7}\,\mathrm{cm^3\,s^{-1}} \quad \text{and}$$
$$\beta = 1.1 \pm 0.2$$

It should be noted that such a strong dependence on temperature is usually found when the dissociative recombination is driven by the indirect mechanism. The measured recombination rate coefficients for DCO^+ ions are somewhat lower than for HCO^+ ions. The obtained $\alpha_{HCO^+}(T)/\alpha_{DCO^+}(T)$ ratio for the temperature range 150–270 K is about ~1.2, and it is in good agreement with the previously obtained value by Poterya et al. [12], and with recently obtained theoretical value by Douguet et al. [15].

We have also studied recombination of HCO^+ using the stationary afterglow apparatus AISA (see description in Refs. [26,40]). The AISA is equipped with mass spectrometer to measure relative densities of ions during the plasma decay. The pressure of the ambient helium in AISA is ~360 Pa. The obtained rate coefficient is $\alpha_{eff}(260\,\mathrm{K}) = (2.0 \pm 0.3) \times 10^{-7}\,\mathrm{cm^3\,s^{-1}}$. The measured time resolved mass spectra confirmed the data obtained from the kinetic model. In the AISA experiments high attention was paid to the suppression of the formation of atomic C^+ ions.

Because of a large disproportion between the recent experimental and theoretical values, the present HCO^+ and DCO^+ FALP and AISA values are plotted in Fig. 7, together with data from other publications. It is easy to see that our results are in a strong agreement with the majority of the previous experimental results in the region, where they overlap. Nevertheless our results are in contradiction with the recent FALP study by Poterya et al. [12] at low temperatures. Additionally, we have not obtained an agreement with recent theoretical values [14,15], which are lower by a factor of at least 10.

4. Conclusions

The recombination of HCO^+ and DCO^+ ions with electrons was studied in cold afterglow plasma in a well-defined FALP experiment. The recombination rate coefficients and their temperature dependencies were measured at temperatures from 150 K up to 270 K. For both ions, the rate coefficients increased as temperatures decreased. Over the studied temper-

ature range the variation of $\alpha_{HCO^+}(T)$ and $\alpha_{DCO^+}(T)$ seems to obey the power law: $\alpha_{HCO^+}(T) = 2.0 \times 10^{-7}\,(T/300)^{-1.3}\ cm^3\ s^{-1}$ and $\alpha_{DCO^+}(T) = 1.7 \times 10^{-7}\,(T/300)^{-1.1}\ cm^3\ s^{-1}$.

The processes in the afterglow were modelled in order to control experimental conditions and to minimise the possible influence of HOC^+ and DOC^+ ions. The measurements were carried out at several buffer gas pressures to check the possibility of a ternary recombination channel; we did not observe a pressure dependence of measured recombination rate coefficients. The obtained rate coefficients agree with values obtained in several afterglow and beam experiments. However they are higher by a factor of ~10 than the recent theoretical values [15]. The measured temperature dependencies are also different from the dependencies observed in the recent experiment of Poterya et al. [12]. In agreement with theory, we observed only a very weak isotopic effect.

Acknowledgements

This paper is dedicated to Zdeněk Herman as an expression of our admiration for him and his scientific work. This work is a part of the research plan MSM 0021620834, financed by the Ministry of Education of the Czech Republic, and was partly supported by GACR (205/05/0390, 202/07/0495, 202/08/H057), by GAUK 53607, GAUK 124707 and GAUK 86908.

References

[1] H. Roberts, E. Herbst, T.J. Millar, Astron. Astrophys. 424 (2004) 905.
[2] T.J. Miller, Planet. Space Sci. 50 (2002) 1189.
[3] E. Herbst, D.E. Woon, Astrophys. J. 463 (1996) L113.
[4] A. Le Padellec, C. Sheehan, D. Talbi, J.B.A. Mitchell, J. Phys. B: At. Mol. Opt. Phys. 30 (1997) 319.
[5] W.D. Geppert, R.D. Thomas, A. Ehlerding, F. Hellberg, F. Österdahl, M. Hamberg, J. Semaniak, V. Zhaunerchyk, M. Kaminska, A. Källberg, A. Paal, M. Larsson, J. Phys.: Conf. Ser. 4 (2005) 26.
[6] M.T. Leu, M.A. Biondi, R. Johnsen, Phys. Rev. A 8 (1973) 420.
[7] T. Amano, J. Chem. Phys. 92 (1990) 6492.
[8] B. Ganguli, M.A. Biondi, R. Johnsen, J.L. Dulaney, Phys. Rev. A 37 (1988) 2543.
[9] N.G. Adams, D. Smith, E. Alge, J. Chem. Phys. 81 (1984) 1778.
[10] D. Smith, P. Spanel, Int. J. Mass Spectrom. Ion Process 129 (1993) 163.
[11] B.R. Rowe, J.C. Gomet, A. Canosa, C. Rebrion, J. Mitchell, J. Chem. Phys. 96 (1992) 1105.
[12] V. Poterya, J.L. McLain, N.G. Adams, L.M. Babcock, J. Phys. Chem. A 109 (2005) 7181.
[13] A. Larson, S. Tonzani, R. Santra, C.H. Greene, J. Phys.: Conf. Ser. 4 (2005) 148.
[14] I.A. Mikhailov, V. Kokoouline, A. Larson, S. Tonzani, C.H. Greene, Phys. Rev. A 74 (2006) 032707.
[15] N. Douguet, V. Kokoouline, C.H. Greene, Phys. Rev. A 77 (2008) 064703.
[16] A.I. Florescu-Mitchell, J.B.A. Mitchell, Phys. Rep.-Rev. Sect. Phys. Lett. 430 (2006) 277.
[17] J. Glosik, I. Korolov, R. Plasil, O. Novotny, T. Kotrik, P. Hlavenka, J. Varju, I.A. Mikhailov, V. Kokoouline, C.H. Greene, Recombination of H^{3+} Ions in the Afterglow of a He–Ar–H_2 Plasma, J. Phys. B (2008), submitted.
[18] V. Kokoouline, C.H. Greene, Phys. Rev. Lett. 90 (2003) 133201; V. Kokoouline, C.H. Greene, Phys. Rev. A 68 (2003) 012703.
[19] M. Larsson, A.E. Orel, Dissociative Recombination of Molecular Ions, Cambridge University Press, Cambridge, 2008.
[20] J. Glosik, R. Plasil, P. Zakouril, V. Poterya, J. Phys. B: At. Mol. Opt. Phys. 34 (2001) 2781.
[21] J. Glosik, R. Plasil, J. Phys. B: At. Mol. Opt. Phys. 33 (2000) 4483.
[22] I. Korolov, J. Varju, T. Kotrik, R. Plasil, M. Hejduk, J. Glosik, Contrib. Plasma Phys. 48 (2008) 521.
[23] J. Glosik, G. Bano, R. Plasil, A. Luca, P. Zakouril, Int. J. Mass Spectrom. 189 (1999) 103.
[24] I. Korolov, R. Plasil, T. Kotrik, P. Dohnal, O. Novotny, J. Glosik, Contrib. Plasma Phys. 48 (2008) 461.
[25] J. Glosik, O. Novotny, A. Pysanenko, P. Zakouril, R. Plasil, P. Kudrna, V. Poterya, Plasma Source Sci. Technol. 12 (4) (2003) S117.
[26] R. Plasil, J. Glosik, V. Poterya, P. Kudrna, J. Rusz, M. Tichy, A. Pysanenko, Int. J. Mass Spectrom. 218 (2002) 105.
[27] J.D. Swift, M.J.R. Schwar, Electrical Probes for Plasma Diagnostics, Iliffe, London, 1970.
[28] D. Trunec, P. Spanel, D. Smith, Chem. Phys. Lett. 372 (2003) 728.
[29] O. Chudacek, P. Kudrna, J. Glosik, M. Sicha, M. Tichy, Contrib. Plasma Phys. 35 (1995) 503.
[30] C.G. Freeman, J.S. Knight, J. Love, M. McEwan, Int. J. Mass Spectrom. Ion Process 80 (1987) 255.
[31] M.A. Smith, S. Schlemmer, J. von Richthofen, D. Gerlich, Astrophys. J. 578 (2002) L87.
[32] R.E. Rosati, M.P. Skrzypkowski, R. Johnsen, M.F. Golde, J. Chem. Phys. 126 (2007) 154302.
[33] I. Dotan, W. Lindinger, J. Chem. Phys. 76 (1982) 4972.
[34] J. Glosik, Int. J. Mass Spectrom. 139 (1994) 15.
[35] H. Villinger, J.H. Futrell, F. Howorka, N. Duric, W. Lindinger, J. Chem. Phys. 76 (1982) 3529.
[36] S. Laube, L. Lehfaoui, B.R. Rowe, J.B.A. Mitchell, J. Phys. B 31 (1998) 4181.
[37] J.B.A. Mitchell, H. Hust, J. Phys. B: At. Mol. Phys. 18 (1985) 547.
[38] H. Liszt, R. Lucas, J.H. Blafl, Astron. Astrophys. 428 (2004) 117.
[39] O. Novotny, R. Plasil, A. Pysanenko, I. Korolov, J. Glosik, J. Phys. B: At. Mol. Opt. Phys. 39 (2006) 2561.
[40] V. Poterya, J. Glosik, R. Plasil, M. Tichy, P. Kudrna, A. Pysanenko, Phys. Rev. Lett. 88 (2002) 044802.
[41] S. Laube, A. Le Padellec, O. Sidko, C. Rebrion-Rowe, J.B.A. Mitchell, B.R. Rowe, J. Phys. B 31 (1998) 2111.